

Stability of AdS in Einstein Gauss Bonnet Gravity

Nils Deppe,^{*} Allison Kolly,[†] Andrew Frey,[‡] and Gabor Kunstatter[§]
Physics Department, University of Winnipeg
(Dated: November 11, 2018)

Recently it has been argued that in Einstein gravity Anti-de Sitter spacetime is unstable against the formation of black holes for a large class of arbitrarily small perturbations. We examine the effects of including a Gauss-Bonnet term. In five dimensions, spherically symmetric Einstein-Gauss-Bonnet gravity has two key features: Choptuik scaling exhibits a radius gap, and the mass function goes to a finite value as the horizon radius vanishes. These suggest that black holes will not form dynamically if the total mass/energy content of the spacetime is too small, thereby restoring the stability of AdS spacetime in this context. We support this claim with numerical simulations and uncover a rich structure in horizon radii and formation times as a function of perturbation amplitude.

INTRODUCTION

Anti-de Sitter (AdS) spacetime has been shown to be unstable against the formation of black holes for a large class of arbitrarily small perturbations, except for specific initial data [1–9]. Given the interpretation of black hole formation as thermalization in the AdS/conformal field theory (CFT) duality, the questions of stability and turbulence of AdS are very important. The instability is apparently due to a subtle interplay of local non-linear dynamics and the non-local kinematical effect of the AdS reflecting boundary. An important question therefore concerns the dependence of the instability and turbulent behaviour on the local dynamics. We investigate the effects of higher curvature terms, which translate to finite N and 't Hooft coupling corrections in the dual CFT.

The most tractable higher curvature term is the Gauss-Bonnet (GB) term, since the equations of motion contain only second derivatives and are readily amenable to a Hamiltonian analysis. Since AdS₅/CFT₄ is a primary case of interest in the context of the AdS/CFT correspondence, we focus on 5D; the GB term, like other curvature-squared terms, is dual to differing a and c central charges in the 4D CFT. As a result, the GB term is commonly studied in the AdS/CFT context.

On the gravity side, the GB term changes the local dynamics in regions of high curvature and radically alters the critical behaviour (Choptuik scaling) of microscopic black hole (BH) formation [10, 11]. One interesting feature of 5D Einstein-Gauss-Bonnet (EGB) gravity is that the horizon radius of a static spherically symmetric BH vanishes for a critical value of the ADM mass, so a BH cannot form dynamically for ADM mass less than this critical value. Such an algebraic mass gap is also present in the 3D Einstein gravity case [12]; nonetheless, 5D EGB gravity differs in that the Riemann tensor is not determined by the Ricci tensor (as opposed to 3D) and the GB term introduces a new length scale.

Due to the reflecting boundary conditions at infinity in AdS spacetime, in the sub-critical region there are two possible endstates: a naked singularity or a quasi-periodic state in which the matter continues to bounce

back and forth. It is important to determine which of these endstates is realized generically.

Of potentially greater interest is whether the GB term stabilizes the spacetime above the algebraic threshold, given evidence [10] that some initial data with super-critical ADM mass still do not form black holes in asymptotically flat spacetime, i.e. that there is a radius gap. This dynamical radius gap is expected to be a feature of EGB in at least all odd dimensions [10] and may also be present in other higher curvature theories. We confirm the presence of a radius gap and observe that in asymptotically AdS spacetime it affects black hole formation even at ADM mass far above the critical value.

In the following we present 5D numerical simulations consistent with the conjecture that the stability of AdS in 5D EGB gravity is restored for arbitrarily small perturbations. In the AdS/CFT correspondence, this would imply that low-energy perturbations of Yang-Mills theories on S^3 need not thermalize when finite N and 't Hooft coupling are taken into account.

ACTION AND EQUATIONS OF MOTION

The action for 5D EGB gravity with cosmological constant minimally coupled to a massless scalar is given by

$$I = \int d^5x \sqrt{-g} \left\{ -\frac{1}{2} \nabla_\mu \psi \nabla^\mu \psi + \frac{1}{2\kappa_5^2} \left(12\lambda + \mathcal{R} + \frac{\lambda_3}{2} [\mathcal{R}^2 - 4\mathcal{R}_{\mu\nu}\mathcal{R}^{\mu\nu} + \mathcal{R}_{\mu\nu\rho\sigma}\mathcal{R}^{\mu\nu\rho\sigma}] \right) \right\}. \quad (1)$$

We will later rescale ψ to remove the Planck scale and numerical factors from the equations of motion. As $R \rightarrow \infty$, any static spherically-symmetric solution asymptotes to AdS with effective cosmological constant $\lambda_{eff} = (1 - \sqrt{1 - 4\lambda\lambda_3})/2\lambda_3$. It proves convenient to use coordinates in which the AdS scale $\lambda_{eff} = 1$.

A Hamiltonian analysis of EGB (and more general Lovelock) gravity in the spherically symmetric context has been carried out in [13–16]; due to the Hamiltonian constraint, the generalized Misner-Sharp mass

function[17]

$$\mathcal{M} = \frac{R^4}{2} \left[\lambda + \frac{(1 - R_{,\mu} R^{,\mu})}{R^2} + \frac{\lambda_3}{R^4} (1 - R_{,\mu} R^{,\mu})^2 \right], \quad (2)$$

gives the energy due to matter within radius R and asymptotes to the ADM mass at $R \rightarrow \infty$ [18]. In terms of the mass function, the horizon condition $(R_{,\mu} R^{,\mu})|_{R_H} = 0$ is

$$\mathcal{M}(R_H) = \frac{1}{2} [\lambda R_H^4 + R_H^2 + \lambda_3], \quad (3)$$

which implies that $R_H \rightarrow 0$ as $\mathcal{M}(R_H) \rightarrow M_{crit} \equiv \lambda_3/2$ even in the dynamical context. This suggests that it is impossible to form a BH when the ADM mass is less than this critical value. This feature is specific to 5D EGB, as it depends critically on the exponent of R_H in the third term of the mass function.

To connect more readily to previous literature, we work in Schwarzschild-like coordinates with metric

$$ds^2 = R_{,x} \left(-Ae^{-2\delta} dt^2 + A^{-1} dx^2 + \frac{R^2}{R_{,x}} d\Omega_3 \right) \quad (4)$$

and spatial coordinate $R = \tan(x)$. In future work, we will consider AdS gravitational collapse in flat-slice coordinates, which are useful for studying scaling and singularity formation since they allow evolution past apparent horizon formation.

The resulting first order equations of motion are

$$\Phi_{,t} = (Ae^{-\delta}\Pi)_{,x} \quad (5)$$

$$\Pi_{,t} = \frac{3}{\sin(x)\cos(x)} Ae^{-\delta}\Phi + (Ae^{-\delta}\Phi)_{,x} \quad (6)$$

$$\delta_{,x} = -\frac{\cos(x)\sin^3(x)(\Pi^2 + \Phi^2)}{[\sin^2(x) - 2\lambda_3(A - \cos^2(x))]} \quad (7)$$

$$\mathcal{M}_{,x} = \frac{A}{2} \tan^3(x)(\Pi^2 + \Phi^2) \quad (8)$$

$$A = 1 + \frac{\sin^2(x)(1 - 2\lambda_3)}{2\lambda_3} \times \left[1 - \sqrt{1 + \frac{8\mathcal{M}\lambda_3}{(1 - 2\lambda_3)^2 \tan^4(x)}} \right]. \quad (9)$$

Here, $\Phi = \psi_{,x}$ and Π is conjugate to ψ . In this parameterization the horizon condition is $A = 0$.

The boundary conditions at the origin are identical to those in asymptotically flat spacetime and are well-known. At infinity, the boundary conditions are

$$\Phi = \rho^3 (\Phi_0 + \Phi_2 \rho^2 + \dots), \quad \Pi = \rho^4 (\Pi_0 + \dots), \quad (10)$$

where $\rho = \pi/2 - x$.

We solve the system (5-9) using the method of lines. [19]. We have verified that our code is consistently convergent, and that conserved quantities, such as the ADM mass, remain fully fifth order accurate throughout simulations. Additionally, we verify that altering parts of the algorithm to higher and lower order methods provides the expected convergence changes

RESULTS

In all simulations we use Gaussian initial data

$$\Phi = 0, \Pi = \frac{2}{\pi} \epsilon \exp \left(- \left(\frac{2 \tan(x)}{\pi \sigma} \right)^2 \right), \sigma = \frac{1}{16}. \quad (11)$$

Fig. 1 shows the horizon radius vs amplitude for 5D Einstein gravity, indicating that our code gives the expected results for long times in this case. Specifically, we see BH formation after the initial pulse bounces off the AdS boundary at infinity, possibly a large number of times. Since the coordinates break down at the horizon, the code signals horizon formation when $A(x, t)$ falls below 2^{7-k} , where k is the exponent in the number of grid points used in the simulation, i.e. $2^{15} + 1$.

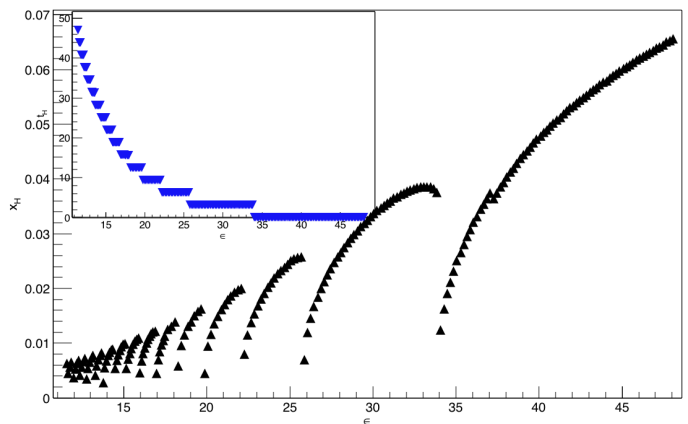


FIG. 1. BH horizon radius on formation vs initial amplitude in Einstein gravity. Inset: horizon formation time vs amplitude.

The inset in Fig. 1 presents a plot of black hole formation time vs amplitude for 5D Einstein gravity. It illustrates that BH formation occurs soon after an integer number of reflections from the AdS boundary (a round-trip time from origin to boundary takes time π). The formation time is approximately piecewise constant, which increases exponentially in each piece as the amplitude decreases.

Fig. 2 shows the effect of introducing a non-zero GB parameter, $\lambda_3 = 0.002$, for the same initial data as above. The figures only cover the range $\epsilon = 36$ to 48 because BH formation for lower amplitudes required many reflections and requires more computation time. The lowest amplitude for which we successfully formed a black hole was $\epsilon = 36$, which required 24 bounces.

The inset of Fig. 2 illustrates the horizon formation time vs amplitude for the same data. It shows that BH's form directly for large amplitudes and transition to forming after one reflection off the boundary for amplitudes $\epsilon \sim 42 - 44$. However, there is rich structure between $\epsilon \sim 44$ and 45.3, where the horizon radius and formation time vary unpredictably.

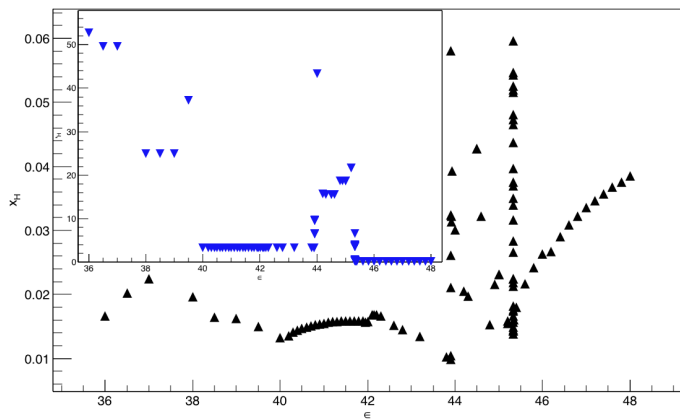


FIG. 2. BH horizon radius on formation vs initial amplitude in EGB gravity, $\lambda_3 = 0.002$. Inset: horizon formation time vs amplitude.

Fig. 3 shows the scaling plot as the critical amplitude $\epsilon = \epsilon^*$ for BH formation is approached after zero and one bounce. Whereas in Einstein gravity these would

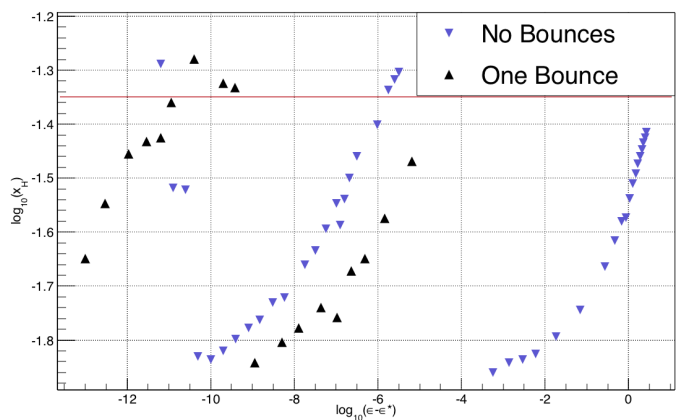


FIG. 3. Scaling of horizon radius at formation after zero and one bounce for $\lambda_3 = 0.002$. Both critical amplitudes are very near 45.33.

be straight lines[20] of slope $\gamma = 0.4131 \pm 0.0001$ [21] corresponding to Choptuik scaling, the graphs level off near $x_H \sim 0.014$ in both cases, suggesting the existence of a radius gap in agreement with [10].

Another feature of both sets of data is a jump in horizon radius as the amplitude is lowered. This can be understood by considering the horizon function, $A(x, t)$. In particular, when the horizon radius gets small, $A(x, t)$ flattens out near horizon formation and additional minima (see Fig. 4) appear. The jump in horizon radius occurs as an outer minimum “overtakes” the inner ones in reaching the value that signals horizon formation in the code first. This indicates that the scalar pulse forms multiple thick shells interior to the outer minimum.

To address the question of the endstate for ADM mass below M_{crit} , we simulated an amplitude $\epsilon = 20$, where

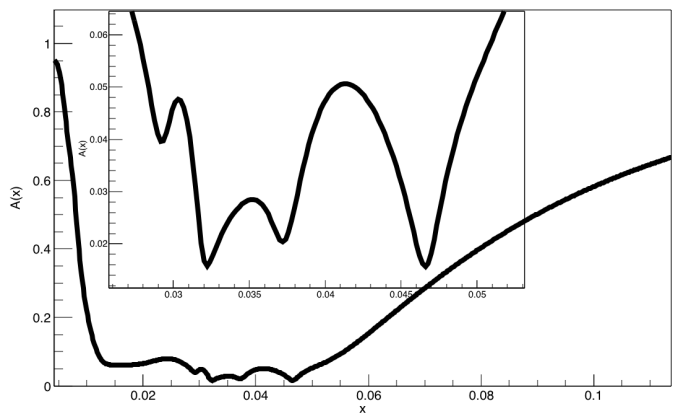


FIG. 4. Metric function A just prior to horizon formation for $\epsilon = 45.33143351875$. Inset: zoomed to show local minima.

$\epsilon_{crit} = 21.86$ corresponds to M_{crit} . Without the GB term this amplitude results in black hole formation after three bounces. In the present case the simulation was continued to $t = 200$, corresponding to over 60 bounces, with no horizon formation. The dynamics of the pulse as it bounces back and forth is quite intricate [22].

Comparison to Einstein gravity is instructive. Fig. 5 graphs Π^2 at the origin, which is proportional to the trace of the stress tensor, for $\epsilon = 12.7$ in Einstein gravity. The tendency of the scalar pulse to get more concentrated, or focused, at the origin after each bounce from the boundary is apparent in the steadily increasing peak value of Π^2 . Fig. 6 graphs Π^2 for $\epsilon = 20$ in EGB gravity. In contrast, the pattern is irregular, and there is no apparent tendency to focus.

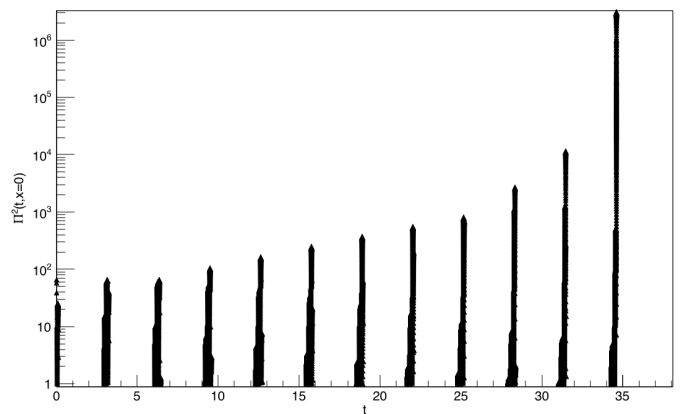


FIG. 5. $\Pi^2(x = 0, t)$ in Einstein gravity for $\epsilon = 12.7$

From the inset in Fig. 6 one can see that there are multiple peaks of $\Pi^2(x = 0)$. This agrees with our observations from animations that the GB term causes the original pulse to break up into multiple smaller pulses, which then propagate through the spacetime. The GB term causes delays in the implosions resulting in a slightly

different phase for the different pulses. We have observed that BH's form when a sufficient number of these pulses are within the horizon radius at the same time. Interestingly, this does not necessarily translate into the curvature being large at the origin.

Additionally, the energy spectrum of the $\epsilon = 20$ pulse shows no evidence of a turbulent cascade of energy to higher frequencies as time passes [22]. This provides some support to the notion that the system settles into a smooth quasi-periodic state, however more simulations are necessary to draw a definitive conclusion.

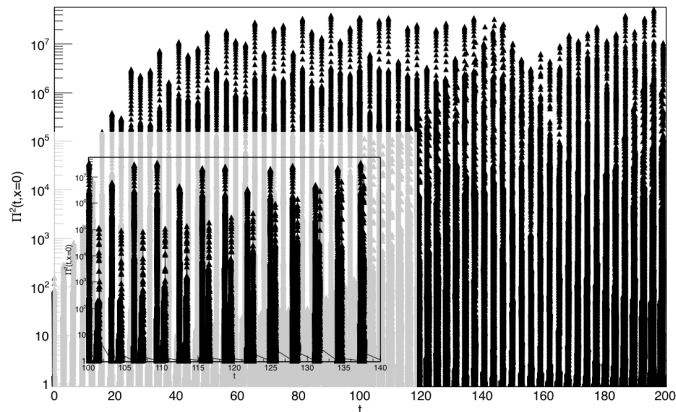


FIG. 6. $\Pi^2(x = 0, t)$ in EGB gravity for $\epsilon = 20$. Inset: zoomed to show peaks with different relative phases.

The above results are in stark contrast with what is seen in the 3D case where an algebraic mass gap is also present. In 3D Einstein gravity, there is no lower bound on the BH radius [23], whereas the BH radius is bounded below in the present case. This behavior seems closely related to the complex structure seen in Fig. 2. Further, the energy spectra for sub-critical collapse in 3D does not share this characteristic behaviour [24, 25].

CONCLUSIONS

We have presented the results of numerical simulations of spherically symmetric massless scalar field collapse in 5D AdS EGB gravity. Our data are consistent with the conjecture that stability against small perturbations is restored. Some speculations are perhaps in order: After each bounce from the boundary, the Einstein term focuses the pulse of matter as it implodes at the origin. On the other hand, the observed dynamical radius gap leads to a defocusing effect that resists BH formation at small horizon radii and allows the matter to travel to the boundary multiple times before BH formation. The defocusing effect is evident in the out-of-phase peaks in $\Pi(x = 0)^2$ seen in Fig. 6 as well as the flattened form of the horizon function (Fig. 4) in EGB gravity. This defocusing in turn affects the time it takes for the pulse

to disperse from the origin. Furthermore, extreme sensitivity of the outcome (BH formation vs dispersion) to initial conditions is a hallmark of critical collapse. This sensitivity along with altered dispersal timescales leads to the complex structure seen in Fig. 2. One can speculate further that the map from amplitude to horizon formation time may evince a fractal structure due to the interplay between Einstein and GB dynamics at the origin. In any case, the data clearly suggest that the GB corrections to short distance dynamics inhibit the formation of black holes and that stability may indeed be restored. Of course, it is much more difficult to prove stability, if indeed that is the case, than instability. We plan a detailed study of these issues in future work.

There are in principle an infinite number of possible higher curvature deformations to Einstein gravity. It is important to ask whether the qualitative features we observe persist in the more general class of deformations. In brief, the suppression of black hole formation in EGB is a consequence of the dynamical radius gap, which is indicative of a non-zero mass critical solution. These are well-known to occur when a new length scale becomes relevant to the dynamics, as invariably happens in gravitational collapse with higher curvature deformations. Thus, we expect the BH suppression to be generic in such theories. Moreover, the sensitivity to initial data of critical collapse in combination with a radius gap should generically lead to complex structure in pulse waveforms and BH formation time in higher-curvature gravities.

In conclusion, our analysis shows that BH formation instabilities in AdS are highly sensitive to small scale dynamics of gravity. Moreover, our results imply finite N and coupling effects modify thermalization in a dual field theory through the AdS/CFT correspondence.

We would like to thank A. Buchel, M. Choptuik, D. Garfinkle, L. Lehner, A. Rostworowski, and T. Taves for useful conversations. This work was funded in part by the Natural Sciences and Engineering Research Council of Canada. Support was also provided by WestGrid (www.westgrid.ca), Compute Canada/Calcul Canada (www.computeCanada.ca), and the Perimeter Institute for Theoretical Physics (funded by Industry Canada and the Province of Ontario Ministry of Research and Innovation).

* nd357@cornell.edu; Current address: Physics Dept., Cornell University

† allisonkolly@gmail.com

‡ a.frey@uwinnipeg.ca

§ g.kunstatter@uwinnipeg.ca

[1] P. Bizoń and A. Rostworowski, *Phys.Rev.Lett.* **107**, 031102 (2011), arXiv:1104.3702 [gr-qc].

[2] J. Jałmużna, A. Rostworowski, and P. Bizoń, *Phys.Rev.* **D84**, 085021 (2011), arXiv:1108.4539 [gr-qc].

- [3] A. Buchel, L. Lehner, and S. L. Liebling, *Phys.Rev.* **D86**, 123011 (2012), arXiv:1210.0890 [gr-qc].
- [4] P. Bizoń and J. Jałmużna, *Phys.Rev.Lett.* **111**, 041102 (2013), arXiv:1306.0317 [gr-qc].
- [5] A. Buchel, S. L. Liebling, and L. Lehner, *Phys.Rev.* **D87**, 123006 (2013), arXiv:1304.4166 [gr-qc].
- [6] M. Maliborski and A. Rostworowski, *Phys.Rev.Lett.* **111**, 051102 (2013), arXiv:1303.3186 [gr-qc].
- [7] M. Maliborski and A. Rostworowski, *International Journal of Modern Physics A* **28**, 1340020 (2013), arXiv:1308.1235.
- [8] M. Maliborski and A. Rostworowski, *Int.J.Mod.Phys.* **A28**, 1340020 (2013), arXiv:1308.1235 [gr-qc].
- [9] M. Maliborski and A. Rostworowski, *Phys.Rev.* **D89**, 124006 (2014), arXiv:1403.5434 [gr-qc].
- [10] N. Deppe, C. D. Leonard, T. Taves, G. Kunstatter, and R. B. Mann, *Phys. Rev. D* **86**, 104011 (2012).
- [11] S. Golod and T. Piran, *Phys.Rev.* **D85**, 104015 (2012), arXiv:1201.6384 [gr-qc].
- [12] M. Banados, C. Teitelboim, and J. Zanelli, *Phys.Rev.Lett.* **69**, 1849 (1992), arXiv:hep-th/9204099 [hep-th].
- [13] J. Louko, J. Z. Simon, and S. N. Winters-Hilt, *Phys.Rev.* **D55**, 3525 (1997), arXiv:gr-qc/9610071 [gr-qc].
- [14] T. Taves, C. Leonard, G. Kunstatter, and R. Mann, *Class.Quant.Grav.* **29**, 015012 (2012), arXiv:1110.1154 [gr-qc].
- [15] G. Kunstatter, T. Taves, and H. Maeda, *Class.Quant.Grav.* **29**, 092001 (2012), arXiv:1201.4904 [gr-qc].
- [16] G. Kunstatter, H. Maeda, and T. Taves, *Class.Quant.Grav.* **30**, 065002 (2013), arXiv:1210.1566 [gr-qc].
- [17] H. Maeda and M. Nozawa, *Physical Review D* **77**, 064031 (2008).
- [18] M. Nozawa and H. Maeda, *Class.Quant.Grav.* **25**, 055009 (2008), arXiv:0710.2709 [gr-qc].
- [19] See Supplemental Material at <http://ion.uwinnipeg.ca/~gkunstat/AdSGB2014SM/SuppMat1410.1869.pdf> for details on the numerical scheme and convergence data.
- [20] M. W. Choptuik, *Phys.Rev.Lett.* **70**, 9 (1993).
- [21] J. Bland and G. Kunstatter, *Phys.Rev.* **D75**, 101501 (2007), arXiv:hep-th/0702226 [hep-th].
- [22] Movies of sub-critical collapse simulations are available at <http://ion.uwinnipeg.ca/~gkunstat/AdSGB2014SM/>.
- [23] F. Pretorius and M. W. Choptuik, *Physical Review D* **62**, 31 (2000), arXiv:0007008 [gr-qc].
- [24] P. Bizoń and J. Jałmużna, *Phys.Rev.Lett.* **111**, 041102 (2013), arXiv:1306.0317 [gr-qc].
- [25] J. Jałmużna, (2013), arXiv:1311.7409 [gr-qc].